HAYATI
Journal of Biosciences

Vol. 30 No. 3, May 2023 576-587
DOI:10.4308/hjb.30.3.576-587
ISSN: 1978-3019
EISSN: 2086-4094

Untargeted LC-QTOF-MS/MS Based Metabolomic Profile Approach of Bacterial Ferment Lysates and Skin Commensal Bacterial Cocktail Ferment Lysates

Ahmad Baikuni[1], Fathan Luthfi Hawari[1], Sutriyo[2], Delly Ramadon[2], Amarila Malik[1*]

[1]*Laboratory of Pharmaceutical Microbiology and Biotechnology, Faculty of Pharmacy, Universitas Indonesia, Depok Campus, Depok 16424, Indonesia*
[2]*Laboratory of Pharmaceutical Technology, Faculty of Pharmacy, Universitas Indonesia, Depok Campus, Depok 16424, Indonesia*

ARTICLE INFO

Article history:
Received September 18, 2022
Received in revised form December 9, 2022
Accepted December 21, 2022

KEYWORDS:
Ferment lysate,
Metabolomic,
Skin microbiome,
Postbiotic,
Untargeted LC-QTOF-MS/MS

ABSTRACT

Microbial therapy has been increasingly developed in the medical and health fields and has triggered advances in the process of formulating skincare products. The skin microbiota becomes the target in the development of active ingredients to produce an optimal effect in the balance of its composition which leads to its usefulness in maintaining skin health and providing protection. Postbiotic bacteria can maintain homeostasis of the skin microbiome so that it has the potential to be used as an active ingredient in Active Pharmaceutical Ingredient (API) in skincare products and have broad benefits due to its various active substances. The aim of this study was to examine the metabolites profile contained in the bacterial fermented lysate fraction, which is also served as a marker in identifying the metabolite variations of the lysate fractions and their API dosage forms. Ferment lysate API preparations were prepared in the form of freeze dried and spray dried. The metabolite profile analysis was carried out using the untargeted LC-QTOF-MS/MS metabolomic approach and multivariate analysis. Result revealed 30 differential features of the putative metabolites, and by performing metabolites annotationfor their bioactivities through intensive literature research, such as antimicrobial, antioxidant, and anti-inflammatory, we elucidated these compounds are discovered in dry form of lysates.

1. Introduction

The development of technology in cosmetics has spawned new innovations, one of which is the trend of using microbial-based therapies. In the last decades, skincare products have used skin microbiomes as its active ingredients, such as skincare industry in England, Korea, and America. Microbial therapy is a new class of active pharmaceutical ingredient in a form of probiotic or postbiotic (Jimenez *et al.* 2019). However, several studies reported the disadvantages of probiotic when applied to individuals with a weak immune system because it can increase the immunogenicity response and is harmful to the function of the skin's protective layer so that currently, active pharmaceutical ingredients tend to use postbiotics as an alternative. Postbiotics have advantages compared to probiotic, such as for skin metabolism, protection from immunogenicity responses and maintain the balance of skin microbiome so that postbiotics have the potential to be used as active ingredients in skincare preparations (Malik 2020). There were several skin microbiomes from Indonesian skin isolated by previous study, those were *Staphylococcus warneri* MBF02-19J, *Staphylococcus hominis* MBF12-19J, *Micrococcus luteus* MBF05-19J, *Bacillus subtilis* MBF10-19J (Khayyira *et al.* 2020). These bacteria were reported to have antimicrobial activity against *Legionella* by producing nukacin ISK-1 and warnericin RK, potential to increase the effectiveness of DNA repair and melanogenesis in melanoma cells, and protect the skin through the production of microbial compounds as were reported (Pauer *et al.* 2019), (Hofer *et al.* 2011), (Hernandez-Valdes *et al.* 2020). The combination of bacteria or bacterial cocktail have been conducted in microbial therapy in a form of postbiotic. The study (Vázquez-

* Corresponding Author
E-mail Address: amarila.malik@ui.ac.id

Castellanos *et al.* 2019) showed that the formulation of double strains of bacteria were more efficient compared to single bacterium and the interaction among bacterial strains can increase the metabolite production and efficacy which are potential as biotherapy. The quality of metabolites produced needs to be monitored to understand its activity and mechanism through metabolomic profile analysis. Recent technological advances have enabled the creation of high throughput profiling of a large number of nontargeted metabolites or metabolomic fingerprinting using liquid chromatography-mass spectrometry (Li *et al.* 2019). Metabolomic profile is a systematic and comprehensive overview of the overall characterization of metabolites or important compounds (Jalu *et al.* 2020). Metabolomic profile analysis can be used to identify and quantify various metabolites to investigate the activity of each bacterium and synergistic effect from bacterial cocktail (Warsito 2018). Various activities of postbiotics and bacterial lysates have been reported, one of which was in the management of skin inflammation associated with photoaging and skin barrier claims such as dry and sensitive skin (Khmaladze *et al.* 2019), reduce vasodilatation, edema, degranulation, mast cells, and TNF-alpha. An assay of trans epidermal water loss showed improvement with application of a postbiotic product (Guéniche *et al.* 2010), a clinical study on the skin of volunteers with mixed atopic dermatitis gave the result that postbiotics have a beneficial effect on skin health and can improve red and itchy skin by increasing the moisture score, inflammation index, and skin brightness score (Ho *et al.* 2021). Therefore, this study analyzed the metabolite profile of single bacterium lysate consist of *Staphylococcus warneri* MBF02-19J, *Staphylococcus hominis* MBF12-19J, *Micrococcus luteus* MBF05-19J, and *Bacillus subtilis* MBF10-19J compared to metabolite profile of cocktail lysate of the four bacterial combinations prepared by freeze drying and spray drying.

2. Materials and Methods

2.1. Bacterial and Subculture Growth Condition

Cryo-stock Staphylococcus hominis MBF12–19J, *Staphylococcus warneri* MBF02–19J, *Bacillus subtilis* MBF10–19J, and *Micrococcus luteus* MBF05–19J were obtained from frozen stock collection in Microbiology and Biotechnology Laboratory, Faculty of Pharmacy, Universitas Indonesia that were isolated by previous study.

Strains were grown in its optimum media; *Staphylococcus hominis* MBF12-19J, *Staphylococcus warneri* MBF02-19J were streaked on Tryptic Soy Agar (TSA), while *Bacillus subtilis* MBF10-19J on Nutrient Agar, and M*icrococcus luteus* MBF05-19J on blood agar, this is the best growth condition for *Micrococcus luteus* MBF05-19J according to our previous studies (Grazia *et al.* 2017; Khayyira *et al.* 2020; Malik *et al.* 2016). All agar cultures were aerobically incubated for 24-48 hours at 37°C. A further subculture step would be conducted by taking pure single colonies using loop and re-scraped on new agar plates. Then, each strain was routinely confirmed by macroscopic and microscopic observation through gram strains (Khayyira *et al.* 2020). All strains were cultured into Tryptic Soy Broth (TSB) production media and the OD_{600} was measured every hour until stationary OD_{600} value is achieved to see the bacteria growth. The data of OD obtained were recorded and then made a growth curve.

2.2. Subculture, Fermentation, and Preparation of Single Bacterial Ferment Lysate

Tryptic Soy Broth was used to culture each strain of bacteria for aerobic enrichment at 37°C without shaking for 24 hours. The reference 0.5 Mc Farland suspension was referred to measure the individual cultures of the strains in the liquid medium, which is equalivalent to the absorbance 0.1±0.05 and the cell density 1.5×10^8 CFU/ml, and by measuring the initial Optical Density (OD_{600}) respectively of each individual culture.

Each strain of bacteria that had been rejuvenated and quality controlled was then fermented in Tryptic Soy Broth (TSB) at 37°C, 50 RPM agitation, and 5% dissolved oxygen aeration with optimum time Micrococcus luteus MBF05-19J = 30 hours; *Bacillus subtilis* MBF10-19J = 7 hours; *Staphylococccus warneri* MBF02-19J = 17 hours; *Staphylococcus hominis* MBF12-19 = 15 hours.

Harvesting was carried out according to the respective growth curve profiles with the optimum OD_{600} by centrifugating to separate the cell pellets and Cell Free Supernatant (CFS). Cell pellets were lysed using an ultrasonicator with duration ratio 0.5 second, 40 cycles, amplitude 75%, 75 seconds duration with 15 seconds pause per cycle. Cell pellets were suspended in a buffer solution, then a protease inhibitor was added before being processed for lysis,

and then lysed on crushed ice. The result of the lysis as fermented lysates was stored at 4°C for further processing for metabolomic analysis.

2.3. Fermentation and Preparation of Bacterial Cocktail Ferment Lysate and Drying Method

The rejuvenation of each bacterial strain was conducted according to their growth curves with the optimum OD_{600}. The bacteria were mixed in the fermenter for 3 hours with the ratio of the composition as reported in our previous study (Baikuni *et al.* 2022), i.e. *Micrococcus luteus* MBF05-19J: *Bacillus subtilis* MBF10-19J: *Staphylococccus warneri* MBF02-19J: *Staphylococcus hominis* MBF12-19J 1 = 1.5:1:0.5:0.5 (K2) or 43%:28%:14.5%:14.5%. Sampling at 1, 2, and 3 hours was carried out to observe the effect of incubation time on the metabolite content, then the bacterial cocktail was harvested and centrifuged. The cell pellets were lysed in the same way as above, and the lysed fractions were dried by freeze drying and spray drying methods. Freeze drying process uses a freeze dryer (Labconco), lyoprotectant inulin 10% was added to the ferment cocktail lysate before being entered into freeze dryer with a temperature of -50°C at a pressure of 0.5-1 mbar for 48 hours and for the Spray Dryer (Buchi), bacterial cocktail ferment lysate was first encapsulated using inulin and maltodextrin 25% before being entered into spray dryer with the inlet temperature of 150°C, outlet temperature of 70°C, nozzle pressure 45 Psi, and flow rate/flow 15%.

2.4. Sample Preparation for Metabolite Analysis

Sample preparation was done by performing an extraction of 1 part of sample dissolved in 4 parts of cold 80% methanol (v/v), which was previously chilled at -20°C for 60 minutes, centrifuged at 14,000 rpm, 4°C, and for 15 minutes. Supernatant resulted was filtered using a 0.22 µm. The storage for all samples was at 4°C within 3 days prior to analyzed (Chan *et al.* 2021).

2.5. Metabolite Analysis by LC-QTOF

All samples were analyzed by LC-QTOF-MS/MS Xevo G2-XS QTOF Quadrupole Time-of-Flight Mass Spectrometry (Waters, USA) with electrospray ionization (ESI) sources under positive and negative modes. In the ESI+ and ESI- modes, the mobile phases A and B were 0,1% formic acid in water and methanol, respectively. The injection volume was 5 L. The separation of chromatograph was reached with an Hss C18 column (2.1 × 100 mm, 1.7 µm; Waters Pacific Pte. Ltd., Singapore), at a flow rate of 0.35 ml/min using the following gradient: Initial 0.300 97.0 3.0 0.0 0.0 97% A for 2 minutes, increases to % B in 8 minutes, 30-80% B in 5 minutes, 80-95% B in 0.5 minute, holds at 95% for 1 minute, then decreases to 5% B in 0.1 minute, and equilibrate at 3% B for 3.5 minutes. Mass ranges obtained were set as 50-1,500 for the TOF and product ion scans. Accumulation time was set at 0.2 second and 0.1 second for TOF and product ion scan. The ESI source parameters were: nebuliser gas and heater set at 50 Psi, curtain gas at 25 Psi, and heater temperature at 500°C. The ion spray voltage was 3,000 and 2,500 V for ESI+ and ESI- modes, respectively. The declustering potential and impact energy were set at 40 V, respectively. The top ten most abundant ions were subjected to the ion scan product where the declustering potential was set at 40 V, and the collision enerfy at 10–70 V for the ESI+ and ESI- modes. The injection sequence consisted of blanks (TSB), single bacteria BS, ML, SH, SW, bacterial cocktail samples with incubation time of 1, 2, 3 hours, blanks (cocktail lysates), bacterial cocktail lysates, blanks (spray and freeze-dried powder), spray dried powder, freeze dried powder. Then, the sample was randomly injected into the system.

2.6. Data Processing and Statistical Analysis

The results of the analysis using LC-QTOF-MS/MS files are converted to mzML files using ProteoWizard (ver. 3.0.23011) to be converted to ABF file using Analysis Base File Converter (ver. 1.3.7815.14260). This was done for the results of ES+ mode and ES- mode respectively. Furthermore, the ABF file of each ES+ and ES- ABF files were analyzed using MS-DIAL (ver. 4.90). Analysis with MS-DIAL already includes peak detection, identification, alignment, and normalization based on the total ion chromatogram (TIC). The results of the analysis are exported to Excel to filter out metabolites that were: duplicated, the intensity less than 3 times the intensity in the blank sample and present in less than 75% of the total sample. After filtering, missing data (data with intensity '0') is replaced with the lowest half of the data from the related metabolite (half of minimum value). The data was then analyzed by heatmap and PCA using R software (ver. 4.2.0). The data is then analyzed in principal components (PCA) using R-Studio (Chan *et al.* 2021). PCA is performed to

observe outliers, assure sample clustering and find inherent sample clustering.

2.7. Putative Annotations of Metabolites

Suspected metabolites are anotated based on retention time and spectral similarity (<15 ppm) by matching against databases such as MassBank (https://massbank.eu/MassBank/), and METLIN (https://metlin.scripps.edu/).

3. Results

3.1. The Confirmation of Bacterial Strains Identity

The confirmation of bacterial strains identity from rejuvenation of frozen stock using macroscopic and microscopic morphological observation is presented in Table 1, and culture for confirmation of growth curve is presented in Figure 1.

3.2. Growth Profile and Fermentation Results

The growth curve of bacterial isolates was made by measuring OD_{600} value every hour until it reached the highest OD_{600} value and entered the stationary phase.

Table 1. Morphological characteristics of isolates

Name of bacteria	Colony shape	Colony color	Gram
S. warneri	Circular	White	+
S. hominis	Circular	White	+
B. subtilis	Rod-like	Brown	+
M. luteus	Circular	Yellow	+

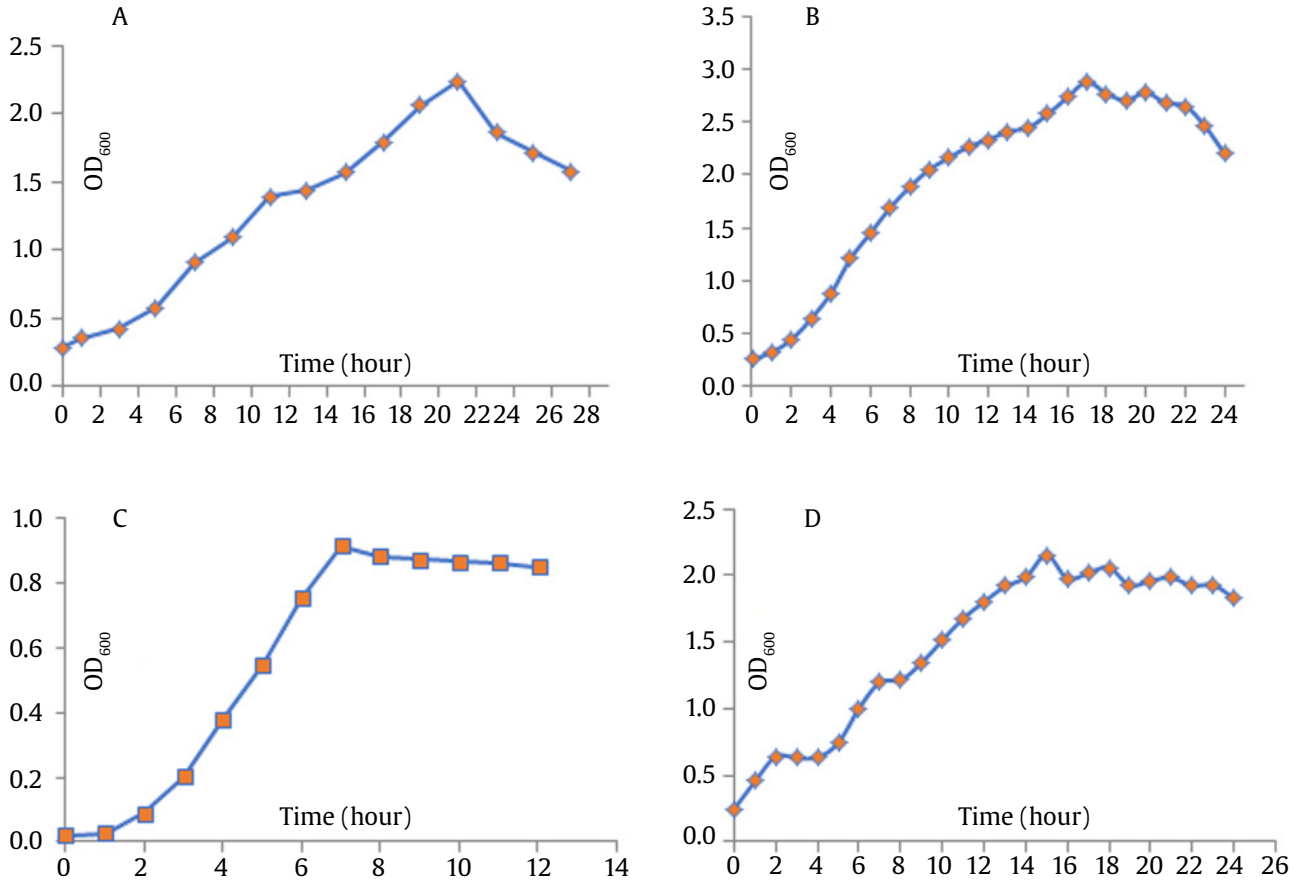

Figure 1. The growth curve of bacterial isolates. Growth curve of *Micrococcus luteus* MBF05-19J with optimum time of 21 hours (A), growth curve of *Staphylococcus warneri* MBF02-19J with optimum time of 17 hours (B), growth curve of *Bacillus subtilis* MBF10-19J with optimum time of 7 hours (C), growth curve of *Staphylococcus hominis* MBF12-19J with optimum time of 15 hours (D)

The observation of growth curve every hour on bacterial isolates in TSB medium showed that final logarithmic phase or exponential phase of Staphylococcus warneri MBF02-19J was at 17 hours, Staphylococcus hominis MBF12-19J at 15 hours, Bacillus subtilis MBF10-19J at 7 hours, *Micrococcus luteus* MBF05-19J at 21 hours. By implementing the growth depiction, the finest result for the fermentation of bacterial cocktail was obtained. The fermentation would be done with 3 hours of incubation time at 37°C, 50 RPM agitation, and 5% dissolved oxygen aeration. 3 hours of incubation was the most proper time for all bacteria to live together and interact in a cocktail form.

3.3. Dry form of Bacterial Cocktail Ferment Lysate

The powder consistencies of bacterial cocktail lysates obtained by both drying processes are shown in Table 2.

3.4. Metabolite Analysis by LC-QTOF-MS-MS

The result obtained from LC-QTOF-MS/MS and all its conversion and analysis can be seen in Supplementary data. In order to obtain the prediction of the metabolites profile existed in various samples, PCA plot score was employed as shown in Figure 2.

Table 2. Powder consistencies of bacterial cocktail ferment lysate from freeze and spray drying

Consistencies	Powder of bacterial cocktail ferment lysate	
	By freeze drying	By spray drying
Types of powder	Coarse powder	Fine powder
Color	Yellowish white	White
Odor	Lysate-like	Lysate-like
Figure	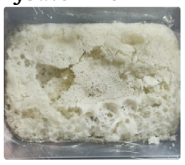	

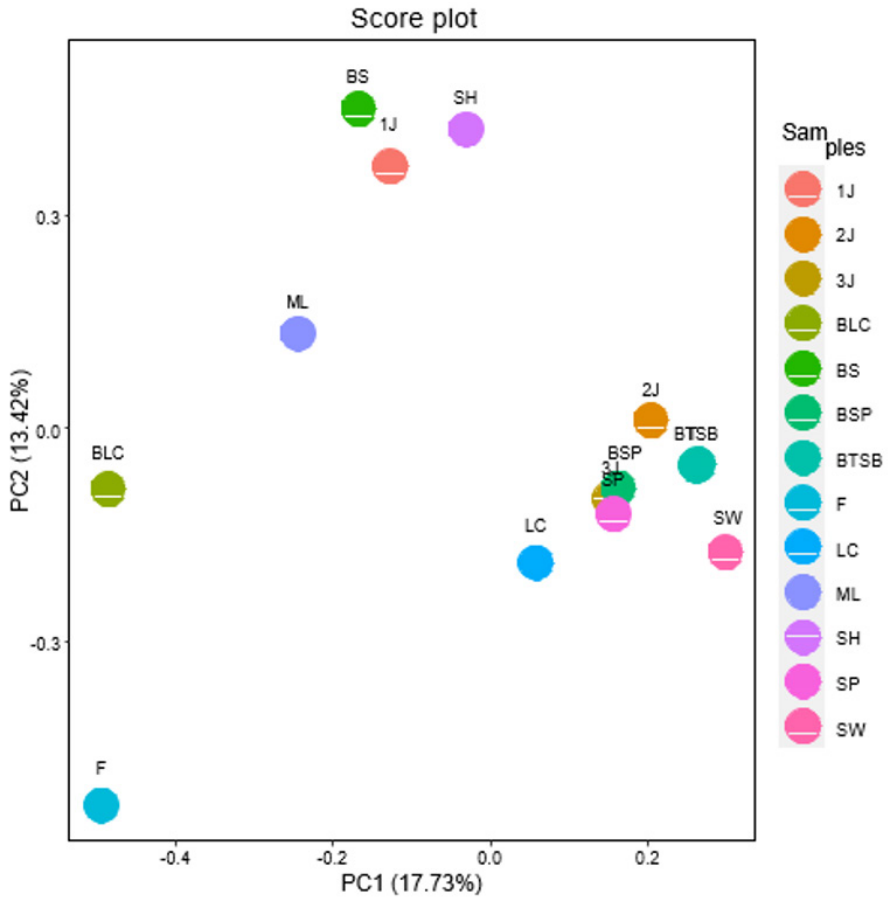

Figure 2. The whole sample PCA score plot. PC1 represented 17.73% samples and PC2 represented 13.42% samples. The coloured ellipses represent for each group. BTSB: blank TSB, BS: *Bacillus subtilis*; ML: *Micrococcus luteus*; SH: *Staphylococcus hominis*: SW: *Staphylococcus warneri*; 1 J: bacterial cocktail samples with incubation time of 1 hour; 2 J: bacterial cocktail samples with incubation time of 2 hour; 3 J: bacterial cocktail samples with incubation time of 3 hours; BLC: blanks cocktail lysates; LC: bacterial cocktail lysates; BSP: blanks (spray and freeze-dried powder); SP: spray dried powder; F: freeze-dried powder

The PCA results showed, that only the spray dry cocktail fermented lysate powder and 3-hour cocktail fermented lysate had the same metabolites due to overlapping PCA plot results.

In addition, a separate PCA analysis was performed between positive mode (ES+) and negative mode (ES-). The first analysis was on the single bacterial fermented lysate group and bacterial cocktail ferment lysate as shown in Figure 3. The second analysis was carried out on the 1 hour, 2 hours, and 3 hours bacterial cocktail ferment lysate group as shown in Figure 4. The last analysis was on the fermented lysate group and bacterial cocktail fermented lysate powder either by freeze or spray dry method as shown in Figure 5.

PCA results showed that each single bacterium (BS, ML, SH, SW) and bacterial cocktail ferment lysates had different metabolite profiles. The results also showed that the long incubation time of the bacterial ferment cocktail and the different drying methods produced different metabolite profiles. Such outcomes were obtained because none of the PCA plots overlapped or were located very closely.

After the clustering and separation confirmed the whole sample PCA score plot, we proceeded to identify feature differentials by performing separate PCA analysis between the ES+ mode and the ES- mode. A total of 935 metabolites and 118 differentiation feature metabolites were preferred in ESI+ and ESI- modes, respectively. In addition, the properties were compared to spectral databases to identify compounds most likely derived from individual bacteria BS, ML, SH, SW, bacterial cocktail samples cultured for 1, 2, and 3 hours, and fermented bacterial cocktail lysates. A total of 30 differential presumptive features properties are described for spray-dried and freeze-dried powders. Table 2 summarizes metabolite experimental mass for charge ratio (m/z), retention time (RT), molecular formula, and MS/MS fragment spectrum.

To reveal metabolites from all samples, we used an LC-QTOF-MS/MS-based non-targeted approach to detect and identify metabolites. A total of 30 differential features of the putative metabolites were described in Table 3. The annotated metabolites suspected in this study have been studied for their bioactivities through literature research, such as antimicrobial, antioxidant, and anti-inflammatory as shown in Figure 6.

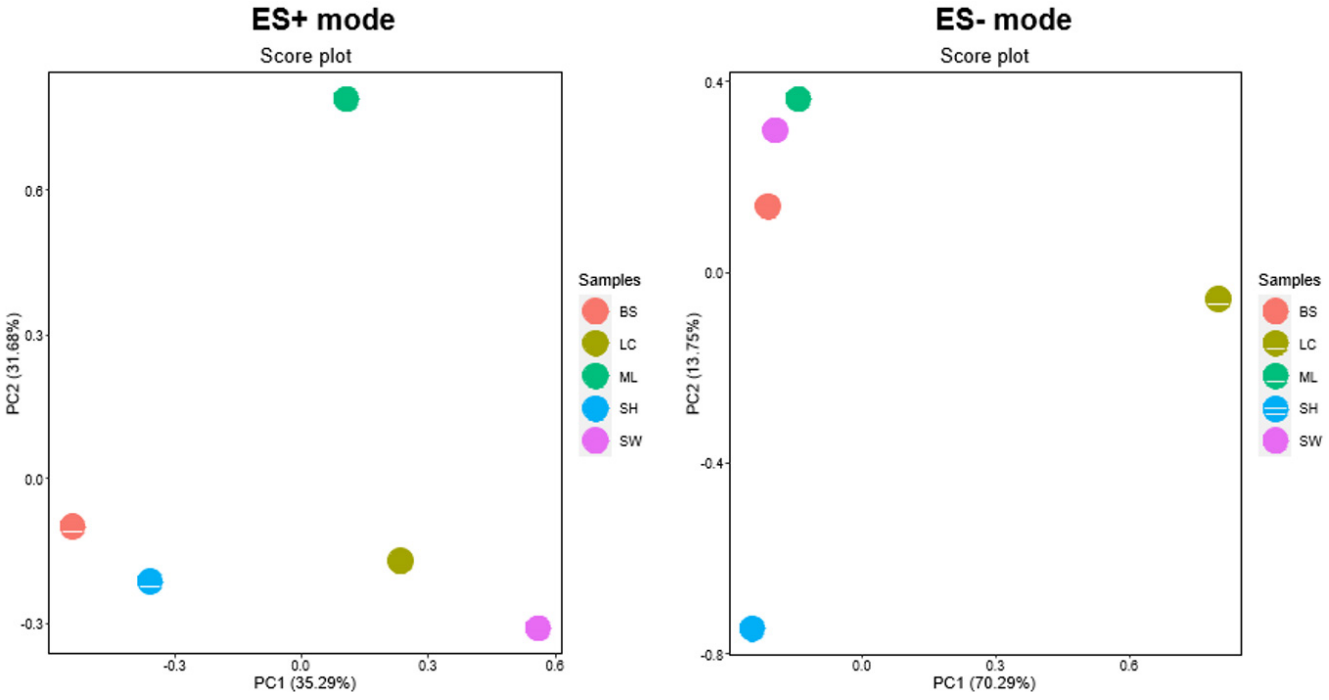

Figure 3. PCA analysis on single bacterial ferment lysates and bacterial cocktail fermented lysates. The coloured ellipses represent each group. BS: *Bacillus subtilis*; ML: *Micrococcus luteus*; SH: *Staphylococcus hominis*: SW: *Staphylococcus warneri*; LC: bacterial cocktail lysates

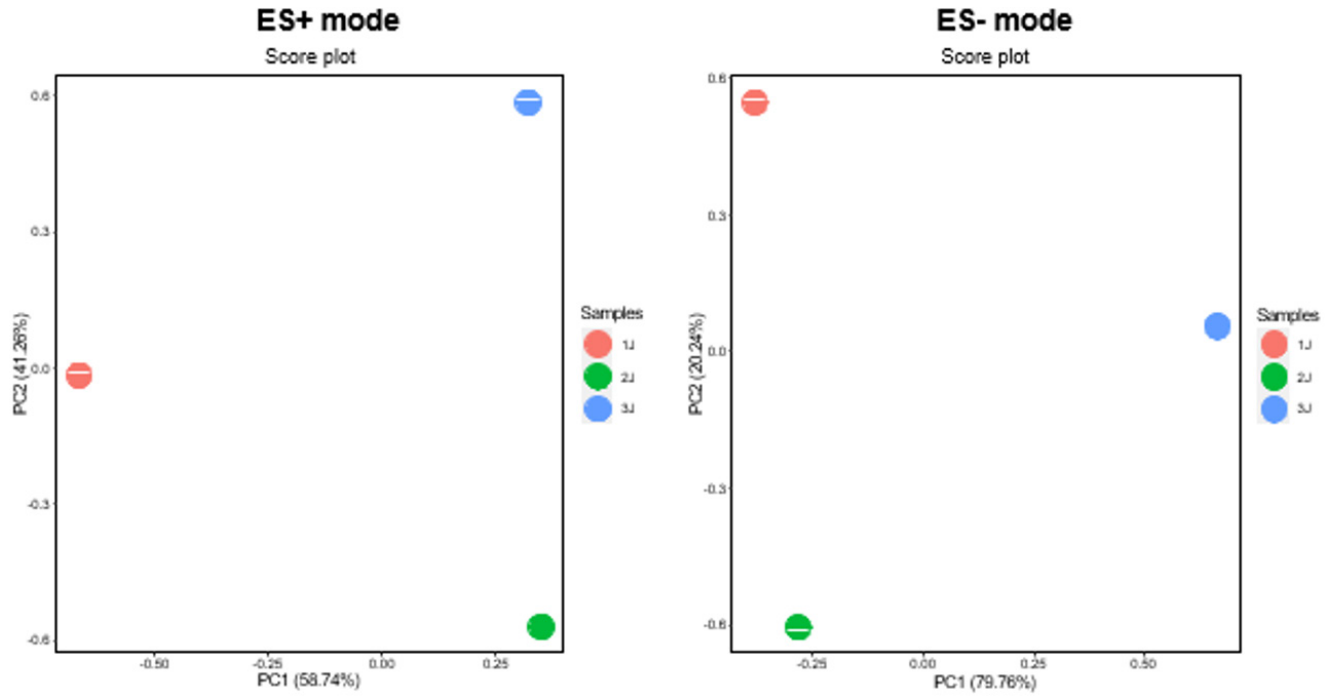

Figure 4. PCA analysis on bacterial cocktail ferment lysate group 1 hour, 2 hours, and 3 hours. The coloured ellipses represent each group. 1 J: bacterial cocktail samples with incubation time of 1 hour; 2 J: bacterial cocktail samples with incubation time of 2 hour; 3 J: bacterial cocktail samples with incubation time of 3 hours

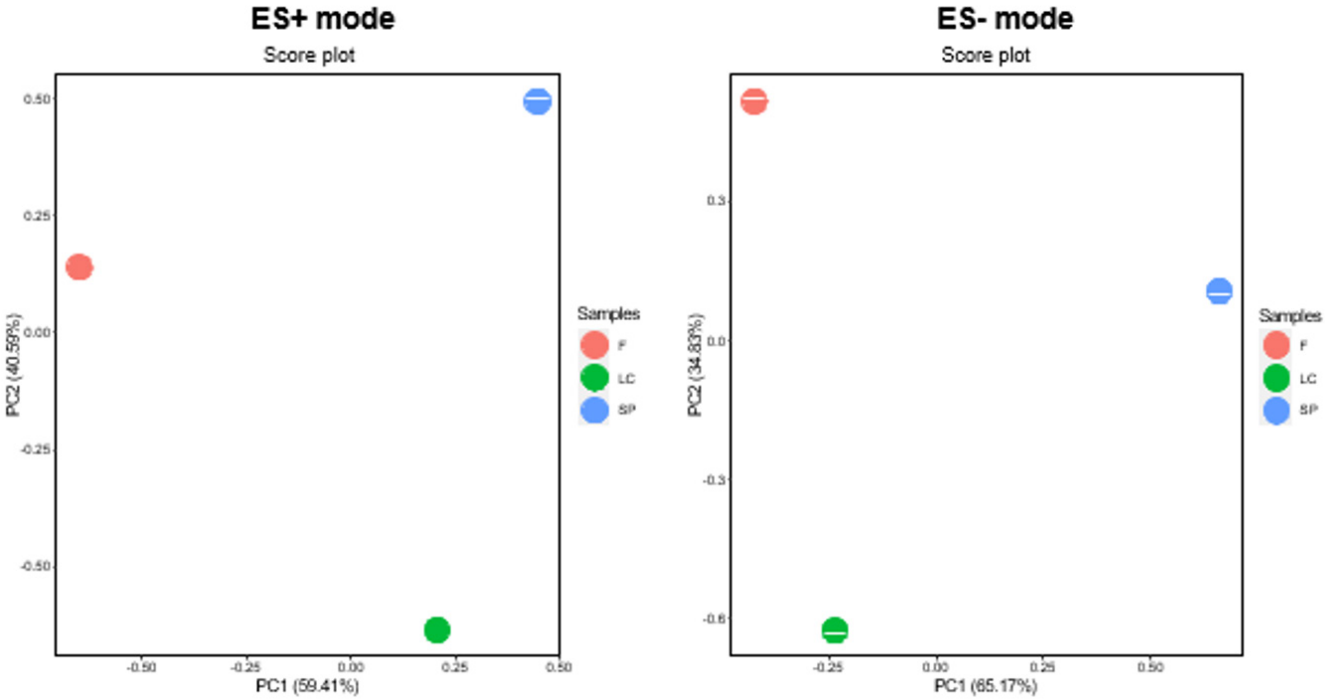

Figure 5. PCA analysis on bacterial cocktail ferment lysate and bacterial cocktail fermented lysate powder. The coloured ellipses represent each group. LC: bacterial cocktail lysates; SP: spray dried powder; F: freeze-dried powder

Table 3. Annotations of suspected metabolites from all samples BS, ML, SH, SW, bacterial cocktail samples with incubation time of 1 hour, 2 hours, 3 hours, bacterial cocktail ferment lysate, spray dried powder, freeze dried powder

Metabolites	m/z	RT (Min)	Adduct	Formula	MS/MS fragments
Pyroglutamic acid	130,051	1,578	[M-2H]-	$C_5H_7NO_3$	41,996, 52,020, 82,030
Chalcone base + 3O, 1MeO, 1Prenyl	353,139	3,364	[M-H]-	$C_{30}H_{22}O_5$	150,024, 300,097, 353,139
Flavone base + 2O, 1MeO, C-Hex	445,115	4,097	[M-H]-	$C_{22}H_{22}O_{10}$	282,048, 297,042, 445,115
Hexose + $C_{10}H_{19}O_2$	395,149	5,207	[M-H]-	$C_{16}H_{30}O_8$	113,027, 161,046, 349,198
Benzyl alcohol + Hex-Hex	431,142	1,263	[M-H]-	$C_{19}H_{28}O_{11}$	101,015, 161,044, 431,142
Licoricesaponin G2	837,275	1,142	[M-2H]2-	$C_{42}H_{62}O_{17}$	469,331, 487,342, 837,275
Ginsenoside Rc	1077.476	0.844	[M-H]-	$C_{53}H_{90}O_{22}$	459,386, 783,486, 945,547
Spirostane -2H, + 1O, O-Pen-dHex	753,381	13.48	[M-2H]2-	$C_{38}H_{60}O_{12}$	707,400, 753,381
Rosmarinic acid	359,081	1,022	[M+K-2H]-	$C_{18}H_{16}O_8$	161,027, 197,047, 359,081
Germinaline	750,286	1,331	[M-H]-	$C_{39}H_{61}NO_{13}$	175,065, 750,286
Soyasapogenol B base + O-HexA +HexA+dHex	953,330	1,177	[M-H]-	$C_{48}H_{74}O_{19}$	339,095, 497,117, 953,330
Corosolic acid	471,261	13,898	[M-H]-	$C_{30}H_{48}O_4$	393,318, 423,327, 471,261
Phenyl-butyryl-glutamine	291,125	1,177	[M-H]-	$C_{15}H_{20}N_2O_4$	119,051, 171,091, 291,125
Flavonol base + 4O, 1MeO, O-Hex, O-Hex, O-Hex	817,259	1,451	[M-H]-	$C_{34}H_{42}O_{23}$	331,046, 493,098, 655,152, 817,259
LPE 18:2	476,359	18,919	[M-H]-	$C_{23}H_{44}NO_7P$	196,037, 279,232, 476,359
Vanillic acid + O-sulfonateHex	409,092	0.913	[M+K-2H]-	$C_{14}H_{18}O_{12}S$	96,957, 241,002, 409,092
Medicagenic acid base + O-Hex	663,207	1,142	[M-H]-	$C_{36}H_{56}O_{11}$	89,024, 439,318, 663,207
Vincanidine	307,154	0.759	[M-H]-	$C_{19}H_{20}N_2O_2$	170,059, 239,092, 307,154
Mitragynine	397,243	11,722	[M-H]-	$C_{23}H_{30}N_2O_4$	174,090, 226,143, 238,142
Abietin	343.14114	3,627	[M+H]+	$C_{16}H_{22}O_8$	365,122, 364,826, 287,001
Paprazine	306.11374	12,430	[M+Na]+	$C_{17}H_{17}NO_3$	147,043, 284,125
Phellopterin	301,.1551	8,076	[M+H]+	$C_{17}H_{16}O_5$	233,044, 245,044, 308,020
Neoandrographolide	503.2641	14,522	[M+2H]2+	$C_{26}H_{40}O_8$	301,307, 289,307, 319,229
Tyramine; PlaSMA ID-59	130.06695	1,835	[M+K]+	$C_8H_{11}NO$	130,063, 122,066, 138,088
Magnolol; PlaSMA ID-1190	267.12311	10,348	[M+H]+	$C_{18}H_{18}O_2$	226,100, 301,074, 197,060
securinine	240.09251	7,377	[M+H]+	$C_{13}H_{15}NO_2$	308,117
arborinine	286.10251	8,751	[M+K]+	$C_{16}H_{15}NO_4$	182,059, 168,079, 196,075
alpha-oxo-1h-indole-3-propanoic acid	204.08833	0.913	[M+H]+	$C_{11}H_9NO_3$	130,065, 172,075, 190,086
Paprazine	306.11374	12,430	[M+Na]+	$C_{17}H_{17}NO_3$	147,043, 284,125, 130,062
Roemerine	280,13391	12,816	[M+H]+	$C_{18}H_{17}NO_2$	279,999, 280,940, 279,789

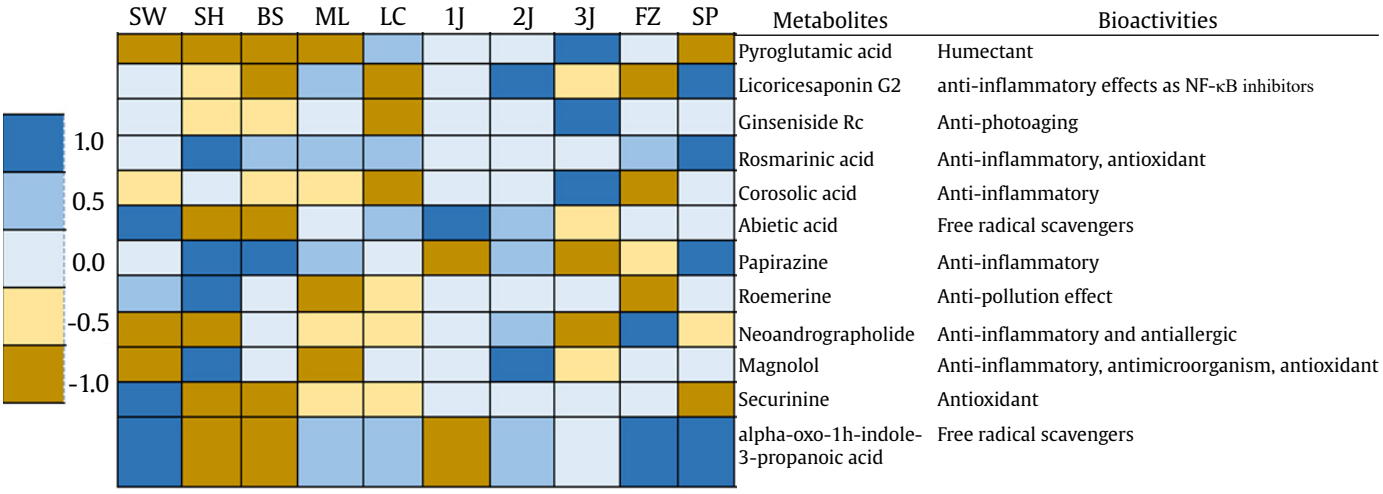

Figure 6. Heatmaps of annotated metabolites suspected of having bioactive properties. The color scale represents the differential intensity of the metabolites, with dark blue and dark brown representing high and low peak intensities, respectively. BS: *Bacillus subtilis*; ML: *Micrococcus luteus*; SH: *Staphylococcus hominis*: SW: *Staphylococcus warneri*; 1J: bacterial cocktail samples with incubation time of 1 hour; 2J: bacterial cocktail samples with incubation time of 2 hour; 3J: bacterial cocktail samples with incubation time of 3 hours; LC: bacterial cocktail lysates; SP: spray dried powder; F: freeze-dried powder

4. Discussion

The growth curve is information about the life phase of the bacteria. Generally, the life phase of bacteria includes condition, log (exponential growth), stationary and dead (Sharah *et al.* 2015). The growth curve for each bacterial strain is intended because each bacterium has a different growth pattern, the length of time it takes to grow or adapt, and the metabolites it produces (Yuliana 2008). The length of the bacterial growth curve is caused by several factors such as the number of cells inoculated, the appropriate physiological and morphological conditions and the cultivation medium used (Sharah *et al.* 2015). By ensuring this growth profile, the amount of each bacteria that will be mixed in cooling the form of a cocktail can be proportional. Proportioned cocktail conditions are designed to allow cocktails to grow and interact by expressing genes close to the state of their products when they are incorporated as components of the microbiome.

Each bacterial isolate that had been rejuvenated and quality controlled and fermented in Tryptic Soy Broth (TSB) media, was harvested at that time based on the respective growth curve profile that had been carried out previously. After each bacteria is harvested, centrifugation is carried out to sell cell pellets and Cell Free Supernatant (CFS) by centrifugation. As for the cocktail bacteria, each isolate was mixed in a 2 liter fermenter for 3 hours. The lysis was carried out using the ultrasonic method. The choice of the lysis method is based on several things, namely analysis of the target molecule, the quality of the final product and the degree of ease of purification (Malik 2020).

The preparation of fermented bacterial lysate in dry form was carried out using freeze drying and spray drying methods. Prior to the drying process, lyoprotectant was added to the fermented lysate to prevent significant aggregation formation caused by the buffer. If aggregation occurs during the lyophilization or drying process, the fermented lysate will not be in the form of powder but in the form of caramel (Kolhe *et al.* 2010). Inulin has been shown to be a therapeutic protection for proteins and viruses during drying and storage. It has also been tested as a protective barrier to maintain the stability of probiotics (yogurt) during freeze drying (Rodríguez Furlán *et al.* 2009).

This type of oligosaccharide is an effective lyoprotectant because it is a stabilizer with a high glass transition temperature (Tg), less number of reducing groups and low crystallization rate, thus extending product shelf life (Rodríguez Furlán *et al.* 2009). In addition, research conducted by Shang *et al.* (2018) reported that inulin has the effect of increasing DPPH antiradical activity.

The universal solvent 80% methanol is used to extract metabolites and precipitate proteins from samples, as it is a common choice for studying non-targeted metabolism due to its non-binding characteristics and wide range of metabolites (e.g.,

amino acids, organic acids, alkaloids, and phenolic compounds). Liquid chromatography methods coupled with high resolution mass spectra such as ultra high performance liquid chromatography coupled with quadrupole time of flight mass spectrometry (UPLC-Q-TOF/MS) are generally used for unbiased investigations of global metabolite profiles due to their high sensitivity and dynamic range large (Chan *et al.* 2021).

The results obtained from LC-QTOF-MS/MS were then traced and analyzed to obtain predictions of the profile of metabolites present in various samples using PCA plot scores. The PCA grouping results showed that only the lysate powder treated by spray dry cocktail and lysate brewed for 3 hours had the same metabolites due to overlapping PCA plot results. In addition, separate PCA analyzes were performed between the positive (ES+) and negative (ES-) modes, the PCA results showed that individual single bacteria (BS, ML, SH, SW) and cocktail cocktail lysates had distinct metabolite profiles. The results also showed that the incubation time of the bacterial excrement cocktail and the different drying methods produced different metabolite profiles. These results were obtained because there were no PCA plots that overlapped or were located very close together.

After clustering and confirmation spoofing of the entire PCA sample score plots, we proceed to identify feature differences. A total of 935 metabolites and 118 metabolite features of differentiation were chosen in the ESI+ and ESI- modes, respectively. Features were compared with the spectral database to identify compounds most likely to be derived from individual bacteria BS, ML, SH, SW, bacterial cocktail samples cultured for 1, 2, and 3 h, and fermented bacterial cocktail lysates. Approximately 30 differentially predicted features are described based on their experimental mass to charge ratio (m/z), retention time (RT), molecular formula, and MS/MS fragment spectra. The results of the annotated metabolites suspected in this study, we have further studied their bioactivity through intensive literature research and have antimicrobial, antioxidant, and anti-inflammatory activities, we explained that these compounds are also found in the form of dry lysates. The focus of this research is to identify metabolites that have activity for skin care. One of the metabolites contained in the sample, namely pyroglutamic acid, has activity as a humectant (National Center for Biotechnology Information 2022a). Although until now there are no clinically approved and/or marketed pharmaceutical products using these active ingredients. Pyroglutamic acid is a naturally occurring amino acid derivative but little information indicates that it can also be formed enzymatically or non-enzymatically (Schilling *et al.* 2008). pyroglutamic acid is generally found in large quantities in brain tissue and other tissues such as skin (National Center for Biotechnology Information 2022a).

Several other metabolites show activity for skin care as an anti-inflammatory including alpha solanine (Hassan *et al.* 2021), licoricesaponin G2 (National Center for Biotechnology Information 2022b), corosolic acid (Sharma *et al.* 2018), paprazine (National Center for Biotechnology Information 2022c), neoandrographolide (Mussard *et al.* 2020), and magnolol (Chen *et al.* 2019). Alpha solanine is also called a glycoalkaloid poison which is found in the genus Solanum such as potatoes, tomatoes and eggplants and is included in the class of saponin compounds (National Center for Biotechnology Information 2022d).

The corosolic acid compound is a common pentacyclic triterpenoid derived from the leaves of banaba or Lagerstroemia speciosa (a tropical plant found in abundance in the Philippines, Vietnam, Malaysia and southern China) (Park and Lee 2011). The compound paprazine or P-coumaroyltyramine is a natural product that can be found in *Ophiopogon japonicus, Polyalthia suberosa*, and other organisms. while the neoandrographolide compound is a natural product derived from Tabernaemontana corymbosa, *Andrographis paniculata*, and P*otamogeton natans.* Magnolol compounds are natural products that can be found in Ma*gnolia garrettii, Illicium simonsii,* and other organisms (National Center for Biotechnology Information 2022c).

Overall, this work demonstrates the appropriateness of LC-QTOF-MS/MS in performing a non-targeted metabolic approach in characterizing the metabolites of bacterial fermented lysates and skin commensal bacterial cocktail lysates. This approach will have broad applicability for uncovering postbiotics or other metabolites, potentially providing a justification for the bioactivity of the metabolites for therapeutic purposes. Nevertheless, further study is needed to measure these postbiotics or metabolites and determine their overall biological relevance, ideally in a clinical setting.

Acknowledgements

This research was supported by a Master Thesis Research grant, Directorate General of Higher Education, Research and Technology, Ministry of Education, Culture, Research and Technology of the Republic of Indonesia, Fiscal Year 2022, No. NKB-892/UN2.RST/HKP.05.00/2022 to A.M., and partially supported by previous research grants received in 2020 to A.M.

References

Baikuni, A., Wanyodiharjo, M.R., Ardiansyah, H., Luthfi, F., 2022. Optimization of cocktail composition and up-scale fermentation process development of four skin commensal bacterial strains. *JIFI.* 20, 113–119.

Chan, M.Z.A., Lau, H., Lim, S.Y., Li, S.F.Y., Liu, S.Q., 2021. Untargeted LC-QTOF-MS/MS based metabolomics approach for revealing bioactive components in probiotic fermented coffee brews. *Food Research International.* 149, 110656. https://doi.org/10.1016/j.foodres.2021.110656

Chen, H., Fu, W., Chen, H., You, S., Liu, X., Yang, Y., Wei, Y., Huang, J., Rui, W., 2019. Magnolol attenuates the inflammation and enhancesphagocytosis through the activation of MAPK, NF-κBsignal pathways *in vitro* and *in vivo*. *Mol. Immunol.* 105, 96-106. https://doi.org/10.1016/j.molimm.2018.11.008.

Grazia, S.E., Sumayyah, S., Sahlan, M., Heng, N.C.K., Malik, A., 2017. Bacteriocin-like inhibitory substance (BLIS) activity of Streptococcus macedonicus MBF10-2 and its synergistic action in combination with antibiotics. *Asian Pacific Journal of Tropical Medicine.* 10, 1140–1145. https://doi.org/10.1016/j.apjtm.2017.11.001

Guéniche, A., Bastien, P., Ovigne, J. M., Kermici, M., Courchay, G., Chevalier, V., Breton, L., Castiel-Higounenc, I., 2010. Bifidobacterium longum lysate, a new ingredient for reactive skin. *Experimental Dermatology*. 19, 1–8. https://doi.org/10.1111/j.1600-0625.2009.00932.x

Hassan, S.H., Gul, S., Zahra, H.S., Maryam, A., Shakir, H.A., Khan, M., Irfan, M., 2021. Alpha solanine: a novel natural bioactive molecule with anticancer effects in multiple human malignancies. *Nutrition and Cancer*. 73, 1541-1552, https://doi.org/10.1080/01635581.2020.1803932

Hernandez-Valdes, J.A., Zhou, L., de Vries, M.P., Kuipers, O.P., 2020. Impact of spatial proximity on territoriality among human skin bacteria. *Npj Biofilms and Microbiomes.* 6, 30. https://doi.org/10.1038/s41522-020-00140-0

Ho, H., Chen, C., Huang, Y., Kuo, Y., Lin, J., 2021. The novel use of postbiotics of TYCA06/AP-32/CP-9 in the amelioration of atopic dermatitis and improvement of skin care-a clinical study. *International Journal of Clinical and Diagnostic Research.* 9, 18–28. https://doi.org/10.12691/ijcdr-9-1-3

Hofer, A., Legat, F.J., Gruber-Wackernagel, A., Quehenberger, F., Wolf, P., 2011. Topical liposomal DNA-repair enzymes in polymorphic light eruption. *Photochemical and Photobiological Sciences*. 10, 1118–1128. https://doi.org/10.1039/c1pp05009e

Jalu, F., Nusantara, P., Putri, S.P., 2020. Metabolomik Mikrobiologi. *Bunga Rampai Forum Peneliti Muda Indonesia*. 77-86.

Jimenez, M., Langer, R., Traverso, G., 2019. Microbial therapeutics: new opportunities for drug delivery. *Journal of Experimental Medicine*. 216, 1005–1009. https://doi.org/10.1084/jem.20190609

Khayyira, A.S., Rosdina, A.E., Irianti, M.I., Malik, A., 2020. Simultaneous profiling and cultivation of the skin microbiome of healthy young adult skin for the development of therapeutic agents. *Heliyon*. 6, e03700. https://doi.org/10.1016/j.heliyon.2020.e03700

Khmaladze, I., Butler, É., Fabre, S., Gillbro, J.M., 2019. *Lactobacillus reuteri* DSM 17938—A comparative study on the effect of probiotics and lysates on human skin. *Experimental Dermatology*. 28, 822–828. https://doi.org/10.1111/exd.13950

Kolhe, P., Amend, E., Singh, S.K., 2010. Impact of freezing on pH of buffered solutions and consequences for monoclonal antibody aggregation. *Biotechnology Progress*. 26, 727–733. https://doi.org/10.1002/btpr.377

Li, X., Zhang, X., Ye, L., Kang, Z., Jia, D., Yang, L., Zhang, B., 2019. LC-MS-based metabolomic approach revealed the significantly different metabolic profiles of five commercial *Truffle* species. *Frontiers in Microbiology*. 10, 1-18. https://doi.org/10.3389/fmicb.2019.02227

Malik, A., Sumayyah, S., Yeh, C., Heng, N.C.K., 2016. Identification and sequence analysis of pWcMBF8-1, a bacteriocin-encoding plasmid from the lactic acid bacterium *Weissella confusa*. *FEMS Microbiology Letters*. 363, 1–8. https://doi.org/10.1093/femsle/fnw059

Malik, A., 2020. *Lisat Fermentasi Mikrobial. In Mikroba dengan Potensi Sebagai Produk Farmasi dan Kesehatan*. IPB Press, Bogor.

Mussard, E., Jousselin, S., Cesaro, A., Legrain, B., Lespessailles, E., Esteve, E., Berteina-Raboin, S., Toumi, H., 2020. *Paniculata paniculata* and its bioactive diterpenoids protect dermal fibroblasts against inflammation and oxidative stress. *Antioxidants.* 9, 432. https://doi.org/10.3390/antiox9050432

National Center for Biotechnology Information, 2022a. Available at: https://pubchem.ncbi.nlm.nih.gov/compound/L-Pyroglutamic-acid. [Date accessed: 7 December 2022]

National Center for Biotechnology Information, 2022b. Available at: https://pubchem.ncbi.nlm.nih.gov/compound/Licoricesaponin-G2. [Date accessed: 7 December 2022]

National Center for Biotechnology Information, 2022c. Available at: https://pubchem.ncbi.nlm.nih.gov/compound/pCoumaroyltyramine. [Date accessed: 7 December 2022]

National Center for Biotechnology Information, 2022d. Available at: https://pubchem.ncbi.nlm.nih.gov/compound/alpha-Solanine. [Date accessed: 7 December 2022]

Pauer, H., Glatthardt, T., Ferreira, N.V., Ferreira, R.B.R., Antunes, L.C.M., 2019. Bioactive molecules of the human microbiome: skin, respiratory tract, intestine. *In: Microbiome and Metabolome in Diagnosis, Therapy, and Other Strategic Applications.* London: Academic Press London, pp. 115–125.

Park, C., Lee, J.S., 2011. Banaba: the natural remedy as antidiabetic drug. *Biomedical Research*. 22, 125-129.

Rodríguez Furlán, L.T., Padilla, A.P., Campderrós, M.E., 2009. Inulin likelyoprotectant ofbovine plasma proteins concentrated by ultrafiltration. *Food Research International.* 43, 788-796. https://doi.org/10.1016/j.foodres.2009.11.015

Shang, H.M., Zhou, H.Z., Yang, J.Y., Li, R., Song, H., Wu, H.X., 2018. *In vitro* and *in vivo* antioxidant activities of inulin. *Plos One*. 13, e0192273. https://doi.org/10.1371/journal.pone.0192273

Schilling, S., Wasternack, C., Demuth, H., 2008. Glutaminyl cyclases from animals and plants: a case of functionally convergent protein evolution. *Biological Chemistry*. 389, 983-991. https://doi.org/10.1515/BC.2008.111

Sharma, H., Kumar, P., Deshmukh, R.R., Bishayee, A., Kumar, S., 2018. Pentacyclic triterpenes: new tools to fight metabolic syndrome. *Phytomedicine*. 50, 166-177. https://doi.org/10.1016/j.phymed.2018.09.011.

Sharah, A., Karnila, R., Desmelati., 2015. Pembuatan kurva pertumbuhan bakteri asam laktat yang di isolasi dari ikan peda kembung (*Rastrelliger* sp.). *Jom*. 2, 1–8.

Vázquez-Castellanos, J.F., Biclot, A., Vrancken, G., Huys, G.R., Raes, J., 2019. Design of synthetic microbial consortia for gut microbiota modulation. *Current Opinion in Pharmacology*. 49, 52–59. https://doi.org/10.1016/j.coph.2019.07.005

Warsito, M.F., 2018. Analisis metabolomik: metode modern dalam pengujian kualitas produk herbal. *BioTrends*. 9, 38–47.

Yuliana, N., 2008. Kinwtika pertumbuhan bakteri asam laktat isolat T5 yang berasal dari tempoyak. *Jurnal Teknologi Industri dan Hasil Pertanian*. 13, 108–116.